

ATMOSPHERIC SCINTILLATION IN RESIDENT SPACE OBJECT PHOTOMETRY

M. Kuhn⁽¹⁾, B. Kieboom⁽¹⁾, G. Cirillo⁽¹⁾, M. Michel⁽¹⁾, and T. Dekorsy⁽²⁾

⁽¹⁾*Airbus Defence & Space, Germany, Email: moritz.kuhn@airbus.com*

⁽²⁾*DLR Institute for Technical Physics (ITP)*

ABSTRACT

In the field of Space Situational Awareness (SSA), precise photometric measurements and light curves are used to characterize resident space objects (RSOs). A contributor to photometric noise that is well known to observers of variable stars or exoplanets, but has so far found little attention among RSO observers, is scintillation caused by atmospheric turbulence.

The present paper sets out to evaluate the impact of scintillation noise on the photometry of RSOs. In particular, unlike most targets of astronomical photometry, RSOs move across the sky, in some cases at considerable angular velocities.

We find that theoretical considerations and computer simulations support the notion that scintillation noise is of relevance for RSO light curve observations, but less so for objects moving at high angular velocities. Attempts to verify this using real-world data from the Airbus Robotic Telescope (ART) yielded no conclusive results, however. We conclude that atmospheric scintillation noise should be kept in mind when aiming for very high precision light curve data of bright RSOs. However, it is likely significantly diminished for fast-moving RSOs in low orbits. A real-world verification of this remains to be done.

Keywords: Photometry, Light Curves, Scintillation.

1. INTRODUCTION

Space-borne assets and infrastructure have become irreplaceable for security and intelligence, scientific research and economic activity. At the same time, near-Earth Space is home to a rapidly growing number of active and defunct satellites, spent rocket stages and other space debris, all collectively referred to as Resident Space Objects (RSOs). Managing this abundance of objects, many of them uncontrolled, and guaranteeing safe and sustainable space operations is the domain of Space Situational Awareness (SSA). This requires information about these RSOs, such as their size, shape or attitude state. One way to obtain this knowledge is through photometry using passive optical sensors. Measuring the brightness of RSOs and its changes over time — called light curves —

allows an observer to recover object information including attitude [1], shape [2] and behaviour [3, 4].

This requires understanding the uncertainties affecting the photometric measurements. Important contributions to photometric uncertainty include Poisson noise from the target and sky background, sensor readout and — particularly for older sensors — dark noise as well as fixed-pattern noise and calibration errors [5]. Another noise component that is important in stellar photometry is scintillation noise, caused by atmospheric turbulence in the light path. In an SSA context, atmospheric scintillation is of relevance in laser ranging [6], but has so far received little attention in the field of RSO photometry. Scintillation noise is often a dominant source of uncertainty in stellar photometry [7]. However, its impact on the photometry of RSOs, which — unlike stars — move across the sky at appreciable angular velocities, has not been investigated to date. Given that some proposed RSO characterization methods rely on high precision photometry (e.g. [4]), this paper aims to offer a preliminary investigation of that question.

The present paper is structured as follows: Section 2 briefly recalls the most important facts and formulae about scintillation in the case of stellar photometry. Section 3 outlines theoretical considerations to adapt these to RSO photometry and describes computer simulations to support them. Section 4 describes our attempts to verify our ideas using real data obtained by the Airbus Robotic Telescope (ART) and the difficulties we faced in the process. Finally, Section 5 summarizes our findings and offers perspectives on possible further work on the topic.

2. ATMOSPHERIC SCINTILLATION NOISE IN PHOTOMETRY

Atmospheric scintillation is not only why stars appear to “twinkle” in the night sky, but also an important source of noise in astronomical photometry. The following is a very brief review of the physics of atmospheric scintillation as it relates to photometry, focusing on the aspects relevant for the further discussion in the context of this paper. For a more complete account of the physical principles and derived statistical properties, we direct the

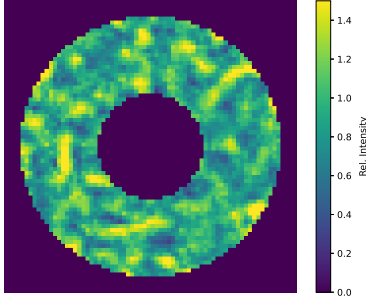


Figure 1: Simulated relative intensity distribution due to atmospheric turbulence in the pupil plane of a 1 m telescope with 40% central obscuration. Speckles of characteristic size $r_F = \sqrt{z\lambda} \approx 0.07$ m can be seen.

reader to a series of exhaustive papers on the topic [8, 9, 10] or a recent, more concise write-up in [11].

Like the related effect of "seeing", which impacts the angular resolution achievable in ground-based astronomy and optical SSA alike, atmospheric scintillation arises from turbulence in the atmosphere. Variations in refractive index due to small temperature differences caused by the turbulence deform the incoming, initially plane wavefronts from extra-atmospheric sources. However, while seeing arises from the phase differences between different sections of the distorted wavefront, scintillation is due to the curvature of the distorted wavefront leading to local focusing or defocusing of the light. This leads to speckles of differing intensity in the pupil plane of a telescope. A simulated example of this is shown in Figure 1. This intensity variation arises from the propagation of the wavefront curvature; it is therefore the high-altitude turbulence, for which the propagation distance is furthest, that mainly causes scintillation. The characteristic size of the speckles seen in Figure 1 is also related to the propagation distance; it is equal to the radius of the first Fresnel zone $r_F = \sqrt{z\lambda}$, with z the propagation distance and λ the wavelength [11].

For telescope apertures D that are large compared to r_F – meaning that the measured intensity is averaged over many speckles – the (normalized) intensity variance of the scintillation is given for short and long exposure times, respectively, by [11]:

$$\sigma_{I,sc}^2 = 17.34D^{-7/3}(\cos \gamma)^{-3} \int_0^\infty h^2 C_n^2(h) dh \quad (1)$$

$$\sigma_{I,le}^2 = 10.66D^{-4/3}t^{-1}(\cos \gamma)^\alpha \int_0^\infty \frac{h^2 C_n^2(h)}{V_\perp(h)} dh \quad (2)$$

with the crossover at approximately the time it takes the speckles to drift across the telescope aperture, assuming a frozen flow (Taylor's hypothesis) [8]. At shorter exposure times, the speckles can be considered frozen in the telescope aperture. More exactly, the exposure time of the switch between short and long exposure regimes is

given by [11]:

$$t_{knee} = 0.62D(\cos \gamma)^{\alpha+3} \int_0^\infty \frac{1}{V_\perp(h)} dh \quad (3)$$

In the previous equations, γ is the horizon distance, t the exposure time, h the height in the atmosphere, $C_n^2(h)$ the turbulence profile and $V_\perp(h)$ the wind velocity profile. The exponent α is usually taken to be 3.5, but in fact depends on the relative geometry of pointing and wind direction [11]. We note that both the long-exposure scintillation strength and the exposure time from which this long-exposure case applies depend inversely on the wind speed profile: intuitively, higher wind speeds cause the intensity speckle pattern to move across the telescope aperture more quickly, so the final measured intensity is averaged over a larger number of speckles.

An alternative measure of the total turbulence strength is the Fried parameter,

$$r_0 = \left(0.423k^2 \sec(\gamma) \int_0^\infty C_n^2(h) dh \right)^{-3/5} \quad (4)$$

with k the wave number. This value, usually on the order of ten centimeters depending on atmospheric conditions, is incidentally also the approximate aperture scale at which the angular resolution of optical telescopes starts being significantly affected by seeing.

An approximate expression for the scintillation noise in the long-exposure regime, called Young's approximation, was introduced in [12] and modified in [11]:

$$\sigma_s = C_Y \cdot 10^{-\frac{5}{2}} D^{-\frac{2}{3}} t^{-\frac{1}{2}} X^{-\frac{3}{2}} \exp\left(-\frac{h_{obs}}{H}\right) \quad (5)$$

with h_{obs} the altitude of the observer, H the scale height of the atmosphere (usually taken to be 8000 m) and C_Y an empirical factor averaging around 1.5 [11, 7]. X is the airmass through which the observation was performed:

$$X = \sec(\gamma)[1 - 0.0012(\sec(\gamma) - 1)] \quad (6)$$

In stellar photometry, this scintillation noise often comes to dominate the total measurement uncertainty, especially for bright sources. For a telescope aperture of 0.5 m, similar to that of ART, scintillation can be the dominant source of uncertainty for targets fainter than $\text{mag}_V = 10.1$ [13]. This makes scintillation a limiting factor in fields such as variable star research or the search for exoplanets.

3. IMPACT ON RSO PHOTOMETRY

3.1. Theoretical Considerations

Given that many RSOs regularly exceed the brightness of $\text{mag}_V = 10.1$ mentioned above, we want to consider the impact of scintillation noise on RSO photometry.

Naively applying Young’s approximation (Equation 5) to RSO observations regularly yields values of several mmag, corresponding to several percent flux uncertainty and dominating the expected uncertainties. However, the most obvious difference between stars and objects in Earth orbit is the latter’s apparent movement across the sky, with LEO objects reaching angular velocities of some degrees per second. We note the wind speed dependence in Equation 2 and Equation 3. We also point out that to first order, there is no difference between the atmospheric turbulence pattern moving relative to the line of sight to target due to the wind and the line of sight moving relative to the turbulence pattern to follow a moving target. There is a higher-order effect in the sense that the turbulence strength is not independent from the wind speed, which is related to the amount of energy available to drive turbulence[7]. This complex relationship is beyond the scope of this work, however.

Keeping in mind the previous point, geometric considerations reveal that the target RSO’s angular velocity ω is equivalent to an additional fictitious “wind speed” contribution of absolute value $\omega \frac{h}{\cos \gamma}$. In the likely case that this additional component is not parallel to the wind velocity, the two must add as vectors. We obtain a modification of Equation 2:

$$\sigma_{I,le}^2 = 10.66 D^{-4/3} t^{-1} (\cos \gamma)^\alpha \int_0^\infty \frac{h^2 C_n^2(h)}{\mathbf{V}_\perp(h) + \mathbf{e}_{V,\omega} \cdot \omega \frac{h}{\cos \gamma}} dh \quad (7)$$

with $\mathbf{e}_{V,\omega}$ the unit vector corresponding to the direction of the additional fictitious wind speed due to the target’s angular velocity. We note that depending on the relative orientation of wind velocity, pointing direction and target angular velocity, the scintillation noise could increase, but for large angular velocities the second term in the denominator will dominate and lead to a decrease of scintillation. Under the simplifying assumption that the turbulence causing scintillation is concentrated in a single turbulent layer of negligible thickness, the integral vanishes; the functional dependence of the scintillation noise on the target’s angular velocity takes the simple form:

$$\sigma_{I,le}^2 \propto \frac{a}{b + \omega} \quad (8)$$

with a, b constants depending on the observation geometry and conditions.

An additional factor that might be expected to affect the impact of scintillation on RSOs is their angular size. A common wisdom among amateur astronomers and stargazers is that while stars can be seen to twinkle, the planets shine steadily under normal conditions. The reason for this is the planet’s angular extent, which causes spatial averaging over a larger area of the turbulent layer, decreasing scintillation. However, objects smaller than about three seconds of arc have been observed to approach the scintillation properties of stars[8, 14]. As only a very small number of RSOs ever exceed this angular

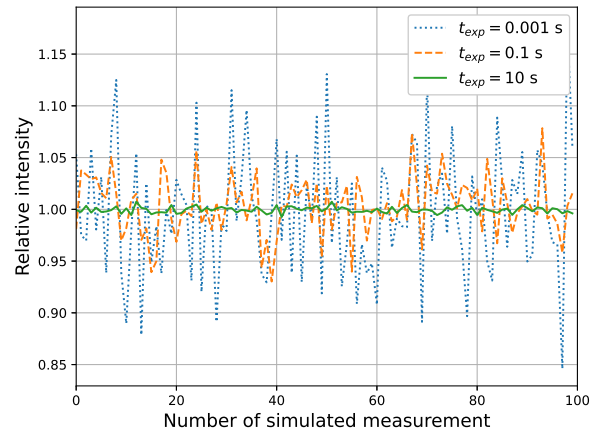


Figure 2: Relative intensity versus number of measurement for three runs of a 100 simulated measurements each. It is apparent that the intensity fluctuates less with longer the exposure time t_{exp} .

size for ground-based observers, we do not consider this aspect further.

3.2. Scintillation Simulation

In order to complement the theoretical considerations above, we simulated photometric measurements affected by atmospheric scintillation in a simple toy model. Similar to [15], we used the *AOtools* python package[16] to simulate a single turbulent layer, or phase screen, at a height of 10 km and moving at a constant, moderate[13] wind speed of 10 m/s. All simulated measurements are performed at zenith. The turbulence strength was characterized by a Fried parameter (see Equation 4) $r_0 = 0.16$ m. For simplicity, we assumed monochromatic light with wavelength $\lambda = 500$ nm. The light is collected by an aperture of 0.4 m diameter with no central obscuration. No other sources of noise were included.

The first set of simulations is intended to explore the exposure time dependence of scintillation. To this end, measurements at different exposure times between 1 ms and 10 s were simulated 100 times each and the standard deviation of the normalized measurements calculated to determine the scintillation noise. Three of these runs of 100 simulated measurements are shown in Figure 2. The results are shown in Figure 3. As expected from Equation 1 and Equation 2, the scintillation noise is constant for short exposures and proportional to $\sqrt{t_{exp}}$ for longer exposures, with the crossover time close to the time $t_{knee} = 0.62D/V_\perp = 0.025$ s predicted by Equation 3. This agreement between the theory and our simple model inspires confidence that, despite the simulation’s relative simplicity, it will be useful in assessing the impact of a target’s movement on scintillation noise.

Next, we simulated targets moving at different angular velocities in the direction parallel to the wind velocity.

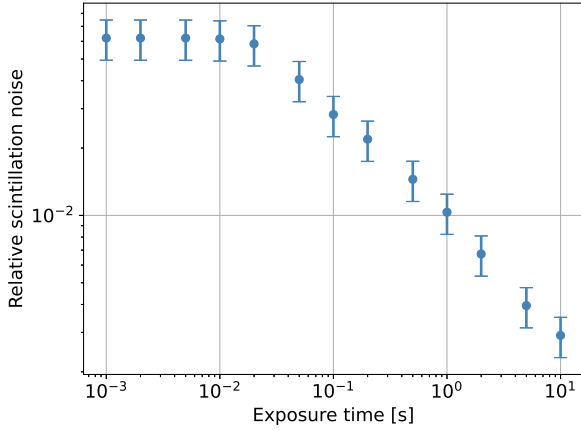


Figure 3: Simulated scintillation intensity at different exposure times. Both the constant scintillation at short exposure times and the inverse square root dependence at longer exposures is clearly visible. See text for a detailed description of the simulation parameters.

An exposure time of 0.1 s was used. Once again, 100 measurements were simulated and the standard deviation for each series calculated to obtain the scintillation noise. The results can be seen in Figure 4. The scintillation noise indeed decreases with increasing angular velocity. Additionally, a function of the form given in Equation 8 fits the simulation results well, lending credence to the ideas developed in Subsection 3.1.

It is worth noting that the magnitude of the wind velocity and its direction relative to the target’s movement effectively sets a lower scale below which the impact of the angular velocity on scintillation is small. This is because for angular velocities below this value, the relative movement between the turbulent atmosphere and the light path to the target is dominated not by the target’s movement, but by the wind, as it is for stationary targets like the fixed stars. For instance, in our simulations the wind speed of 10 m/s at a height of 10 km corresponds to an angular velocity of 1 mrad, i.e. about 0.06° or $200''/s$; for off-zenith pointings, the exact value would depend on the relative geometry of pointing and wind direction. $200''/s$ is similar to the angular velocities of some MEO satellites – for example, the LAGEOS geodetic satellites – and significantly larger than that of GNSS satellites or objects in GEO.

4. REAL-WORLD DATA

To test the angular velocity dependence of the scintillation noise for RSO on real-world photometric data we use the Airbus Robotic Telescope (ART). ART is a 40 cm aperture telescope with a $3.18^\circ \times 2.39^\circ$ field-of-view, using a modern 150 megapixel CMOS sensor. Each image is corrected with a dark and (sky) flat frame, after which the photometric measurements are obtained using

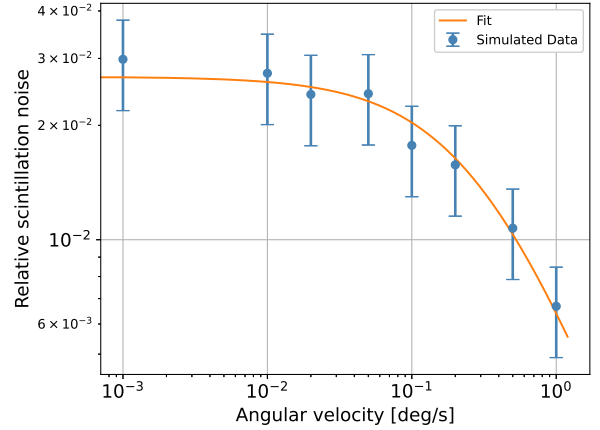


Figure 4: Simulated scintillation intensity at different angular velocities, assuming a 10 m/s wind speed in the turbulence in the direction against the object’s movement. A function of the form of Eq. 8 fits the points well. See text for a detailed description of the simulation parameters.

aperture photometry. To estimate the scintillation noise, consider first the total variance of a photometric measurement[5]:

$$\sigma^2 = n_{\text{ap}} \left(1 + \frac{n_{\text{ap}}}{n_{\text{an}}} \right) (N_B + N_D + \sigma_R^2 + G^2 \sigma_f^2) + \sigma_S^2 + N_* \quad (9)$$

where N_* are the total number of electrons from the object being measured, n_{ap} the number of pixels in the photometric aperture, n_{an} the number of pixels in the photometric annulus, N_B the mean background electrons per pixel, N_D the mean dark current electrons per pixel, σ_R the read noise per pixel, G and σ_f the camera gain and A/D noise, and σ_S the scintillation noise. The number of dark current electrons N_D for the instrument used in this experiment are measured to average up to approximately 0.02 electrons for exposures of 5 seconds, and are therefore neglected. The A/D conversion error is $G^2 \sigma_f^2 = (0.76 \sqrt{1/16})^2 \approx 0.04$ and is also neglected.

For a given light curve, the total variance σ^2 for each measurement can be obtained by subtracting the true light curve from the measured light curve. The true light curve is not known, and must be estimated. In this work, we fit a smooth spline to light curves associated with RSOs and for stars the mean value is used. Figure 5 shows the measured and fit light curves for the star HD 96819 (top) and the RSO 32276 Starlink (bottom).

To estimate the scintillation noise, we subtract from the estimated total variance $\hat{\sigma}^2$ the contribution of the Poisson and read noise, which we denote as $\hat{\sigma}_P$ and is readily computed using the camera properties and the measured background and signal. The scintillation noise

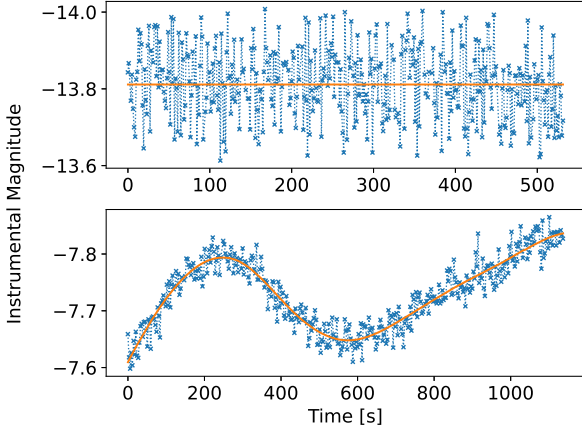


Figure 5: measured and fit light curves for the star HD 96819 (top) and the RSO 32276 Starlink (bottom).

estimate is then given by $\hat{\sigma}_S = \sqrt{\hat{\sigma} - \hat{\sigma}_P}$.

To verify the validity of the method, we measured the light curves of several stars at different elevations and exposure times spanning two nights, each light curve consisting of approximately 350 and 480 measurements, respectively. Figure 6 shows the relative scintillation noise for each star at different airmass levels and a fixed exposure time of 0.1 s. The expected behaviour is observed, namely that the scintillation noise tends to increase for increasing airmass.

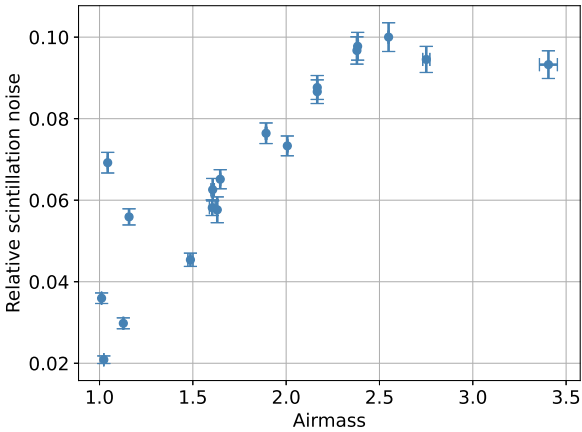


Figure 6: Scintillation noise for different stars at different levels of airmass.

Figure 7 shows the relative scintillation noise of two different stars for different exposure times at an airmass of roughly 1.65. Overall, the scintillation noise decreases with increasing exposure time, as expected. The observed slope in the log-log plot is compatible with the inverse square root dependence predicted by Equation 2.

The variance in the data may be explained by changing atmospheric conditions. The measurements were taken

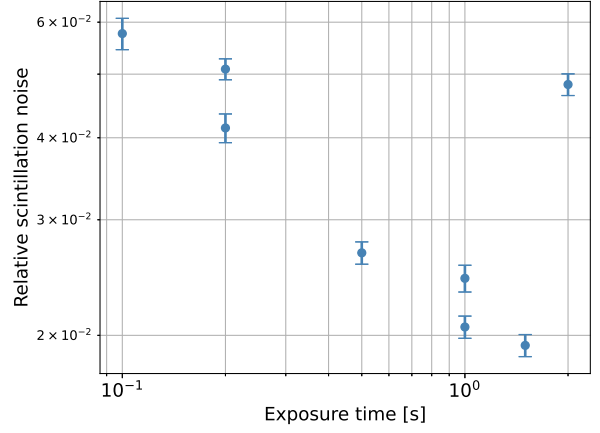


Figure 7: Scintillation noise of two different stars at approximately 1.65 airmass for different exposure times.

at different times and are separated by up to more than a day. In such time spans, the atmospheric conditions can change significantly [11, 7]. Similarly, such changes may also occur at larger spatial scales (e.g. from the western to the eastern horizon). The different atmospheric conditions can cause different levels of scintillation noise contribution [8].

To estimate the scintillation noise for RSOs at different angular velocities we resorted to the use of archival data spanning all of 2024, as the weather did not permit the retrieval of a dedicated RSO data set. The results of this experiment remain inconclusive and are not shown. There are two main reasons why measuring the scintillation noise for RSOs is more difficult. Firstly, extracting the total variance estimate from a RSO light curve is more difficult, it is sometimes hard to distinguish features of the true light curve from noise, for instance, when a relatively high frequency component of the signal is under sampled. The second reason is that atmospheric conditions between measurements can vary significantly over time, necessitating the observation of different objects relatively closely spaced in time. The set of suitable objects for scintillation noise estimation that can be observed using ART is limited, however, due to objects not being bright enough or having a too short of a measured light curve. The data set used for analysis in this case, did not satisfy this requirement, and proved insufficient. In order to therefore test the hypothesised dependency of the scintillation noise on the angular velocity, a dedicated data set of RSOs needs to be obtained.

5. CONCLUSIONS

The present paper set out to investigate the impact of scintillation noise on photometric measurements of RSOs. A particular focus was placed on how the scintillation noise is affected by the fast apparent movement of RSOs – in contrast to the fixed stars that are often targets of astro-

nomical photometry, where scintillation noise is often the dominant source of measurement uncertainty.

We found that for fast-moving RSOs, scintillation noise is generally expected to decrease. On the other hand, the situation is more complex for slower objects, for which the movement of the scintillation pattern is dominated by the wind velocity rather than by the object's movement. Simulations of a simple model of scintillations were found to agree with these predictions. We therefore conclude that scintillation noise should be kept in mind by RSO observers interested in precise photometry. This is especially the case for targets that are fairly bright, but not too fast and targets observed at high airmass.

We also attempted to validate our findings using real-world measurements from ART. This is despite the instrument not being designed for this work, with a relatively slow frame rate incapable of sampling the higher frequency parts of atmospheric scintillation and no way of ascertaining the high-altitude wind speed or turbulence strength at the observatory site. Observations of stars at different exposure times and airmasses indeed conform to the theoretical expectations, inspiring confidence in our data reduction methods. However, we were unable to conduct a planned dedicated observation campaign to investigate scintillation noise in RSO photometry due to unfavourable weather conditions and observational constraints. Attempts to use archival data from 2024 instead yielded no conclusive results regarding e.g. a dependence of scintillation noise on airmass, exposure time or angular velocity. This may be at least in part due to variations in atmospheric conditions over the course of the year.

For this reason, a validation of the results presented in this paper using real-world data still remains to be done. This would require a sufficient amount of photometric data collected from bright RSOs moving at different angular velocities. Ideally, however, this would be done using an instrument or set of instruments more suited to these measurements than ART, including particularly the ability to measure and record local atmospheric conditions at the time of observation. An investigation of the variation of scintillation noise at very large angular scales, relevant in the case of RSOs crossing large parts of the sky in a short time, would also be interesting. To support such work, more sophisticated simulations covering the entire imaging scenario would be helpful.

REFERENCES

1. Wetterer, C. J. and Jah, M. (2009). "Attitude Determination from Light Curves". *Journal of Guidance, Control, and Dynamics* 32.5, pp. 1648–1651. DOI: 10 . 2514/1 . 44254.
2. Furfaro, R., Linares, R., and Reddy, V. (2019). "Shape Identification of Space Objects via Light Curve Inversion using Deep Learning Models". Advanced Maui Optical and Space Surveillance Technologies Conference. Hawaii, p. 17.

3. Coder, R. D., Holzinger, M. J., and Jah, M. K. (2018). "Space-Object Active Control Mode Inference Using Light Curve Inversion". *Journal of Guidance, Control, and Dynamics* 41.1, pp. 88–100. DOI: 10 . 2514/1 . G002224.
4. Spurbeck, J. et al. (2021). "Near Real Time Satellite Event Detection, Characterization, and Operational Assessment Via the Exploitation of Remote Photoacoustic Signatures". *The Journal of the Astronautical Sciences* 68.1, pp. 197–224. DOI: 10 . 1007 / s40295-021-00252-5.
5. Castro, P. J. et al. (2020). "Calculating Photometric Uncertainty". Advanced Maui Optical and Space Surveillance Technologies Conference.
6. Degnan, J. J. (2016). "An Upgraded SGSLR Link Analysis Which Includes the Effects of Atmospheric Scintillation and Target Speckle". 20th International Workshop on Laser Ranging. Potsdam.
7. O'Brien, S. M. et al. (2021). "Scintillation-limited photometry with the 20-cm NGTS telescopes at Paranal Observatory". *Monthly Notices of the Royal Astronomical Society* 509.4, pp. 6111–6118. DOI: 10 . 1093 / mnras / stab3399.
8. Dravins, D. et al. (1997a). "Atmospheric Intensity Scintillation of Stars. I. Statistical Distributions and Temporal Properties". *Publications of the Astronomical Society of the Pacific* 109, p. 173. DOI: 10 . 1086 / 133872.
9. Dravins, D. et al. (1997b). "Atmospheric Intensity Scintillation of Stars. II. Dependence on Optical Wavelength". *Publications of the Astronomical Society of the Pacific* 109, p. 725. DOI: 10 . 1086 / 133937.
10. Dravins, D. et al. (1998). "Atmospheric Intensity Scintillation of Stars. III. Effects for Different Telescope Apertures". *Publications of the Astronomical Society of the Pacific* 110.747, pp. 610–633. DOI: 10 . 1086 / 316161.
11. Osborn, J. et al. (2015). "Atmospheric scintillation in astronomical photometry". *Monthly Notices of the Royal Astronomical Society* 452.2, pp. 1707–1716. DOI: 10 . 1093 / mnras / stv1400.
12. Young, A. T. (1967). "Photometric error analysis. VI. Confirmation of Reiger's theory of scintillation". *The Astronomical Journal* 72, p. 747. DOI: 10 . 1086 / 110303.
13. Föhring, D. et al. (2019). "Atmospheric scintillation noise in ground-based exoplanet photometry". *Monthly Notices of the Royal Astronomical Society* 489.4, pp. 5098–5108. DOI: 10 . 1093 / mnras / stz2444.
14. Young, A. T. (1969). "Photometric Error Analysis. VIII. the Temporal Power Spectrum of Scintillation". *Appl. Opt.* 5, pp. 869–885. DOI: 10 . 1364 / AO . 8 . 000869.
15. Hartley, K. E. et al. (2023). "Optical sparse telescope arrays and scintillation noise". *Monthly Notices of the Royal Astronomical Society* 526.1, pp. 1235–1245. DOI: 10 . 1093 / mnras / stad2835.
16. Townson, M. J. et al. (2019). "AOTools: a Python package for adaptive optics modelling and analysis". *Optics Express* 27.22, p. 31316. DOI: 10 . 1364 / OE . 27 . 031316.